Plant Mol Biol Rep (2016) 34:748–760
DOI 10.1007/s11105-015-0962-y

ORIGINAL PAPER

Disruption of *OsARF19* is Critical for Floral Organ Development and Plant Architecture in Rice (*Oryza sativa* L.)

Shengzhong Zhang[1] · Tao Wu[1] · Shijia Liu[1] · Xi Liu[1] · Ling Jiang[1] · Jianmin Wan[1,2]

Published online: 25 November 2015

Abstract Floral organ development is fundamentally important to plant reproduction and seed quality, yet its underlying regulatory mechanisms are still largely unknown, especially in crop plants. In this study, we characterized rice null mutant *osarf19*, which was isolated from a T-DNA insertion pool. The mutant displayed three types of abnormal florets: an enlarged and degenerated palea, and an additional lemma. It also showed enlarged plant architecture, including elongated basal internodes and leaves. Cellular morphology and quantitative real-time PCR (qRT-PCR) analyses showed that cell elongation caused the enlarged organs. Transgenic RNA interference (RNAi) lines of *OsARF19* had similar phenotypes to the *osarf19* mutant, confirming the role of *OsARF19* in floral and vegetative organ development. *OsARF19* is expressed in various tissues, especially young panicles and basal internodes, which are elongated. *OsARF19* was induced by IAA (indole-3-acetic acid) treatment and functioned in the nucleus. By qRT-PCR analysis, we found that disruption of *OsARF19* increases expression levels of *OsYUCCA* and *OsPIN* family members, while reducing *OsGHs* transcription activity. The high auxin performance greatly upregulated two floral organ regulators, *OsMADS29* and *OsMADS22*, possibly responsible for palea abnormalities in *osarf19*. Our data provide new knowledge on the mechanisms of floral organ development, as well as possibilities in breeding for ideal plant architecture.

Keywords ARF19 · Floral organs · Cell length · *Oryza sativa* · Plant architecture

Abbreviations

ARF	Auxin response factor
var	Variety
cv	Cultivar
FLS	Flanking sequence
qRT-PCR	Quantitative real-time PCR
GFP	Green fluorescent protein
GUS	Beta-glucuronidase
IAA	Indole-3-acetic acid

Introduction

The initiation and differentiation of floral organs are of fundamental importance in the plant life cycle. In rice, normal development of floral organs is essential for reproduction and seed quality. Multiple genes influence floret formation in rice, and most of them are classified into groups based on the ABCDE model, that was originally derived from the ABC model proposed for *Arabidopsis* (Krizek and Fletcher 2005; Theissen 2001; Thompson and Hake 2009). *RAP1A* and *RAP1B* that belong to Class A (Moon et al. 1999) affect palea development. *OsMADS2* and *OsMADS16*, Class B genes, control formation of the lodicule and paleolate (Xiao et al. 2003; Yadav et al. 2007). *OsMADS3* and *OsMADS58* in class

Electronic supplementary material The online version of this article (doi:10.1007/s11105-015-0962-y) contains supplementary material, which is available to authorized users.

✉ Ling Jiang
jiangling@njau.edu.cn

✉ Jianmin Wan
wanjm@njau.edu.cn

[1] State Key Laboratory for Crop Genetics and Germplasm Enhancement, Jiangsu Plant Gene Engineering Research Center, Nanjing Agricultural University, Nanjing 210095, China

[2] National Key Facility for Crop Gene Resources and Genetic Improvement, Institute of Crop Science, Chinese Academy of Agricultural Sciences, Beijing 100081, China

C determine the identities of pistils and carpel (Yamaguchi et al. 2006; Li et al. 2011a). OsMADS13, a Class D protein, plays a role in ovule development (Dreni et al. 2007). *OsMADS1*, a Class E gene, functions in balancing meristem growth, lateral organ differentiation, and determinacy (Khanday et al. 2013). In addition to the ABCDE model, many other factors such as phytohormones also affect floret development. These include auxins (McSteen 2010), cytokinins (Khanday et al. 2013), and jasmonic acid (Cai et al. 2014).

Auxin, a morphogen-like hormone, regulates multiple aspects of plant growth and development, including leaf development, apical dominance, shoot and root elongation, lateral root initiation, and vascular differentiation (Benkova et al. 2003). Auxin responses are mediated by a class of transcription factors called auxin response factors (ARFs), which are repressed by Aux/IAA proteins in the absence of auxin (Guilfoyle and Hagen 2007).

In previous studies, the biological functions of several ARFs were reported in *Arabidopsis* (*Arabidopsis thaliana* L.) and rice (*Oryza sativa* L.). For example, MP/ARF5 can affect leaf initiation, embryo patterning, flower patterning, and vascular differentiation (Aida et al. 2002; Garrett et al. 2012; Hardtke and Berleth 1998; Hardtke et al. 2004; Przemeck et al. 1996). NPH4/ARF7 and ARF19 affect leaf expansion and promote lateral root formation via direct activation of LBD/ASL genes in *Arabidopsis* (Okushima et al. 2007; Wilmoth et al. 2005). Besides, ARF19 can also bind to the promoter of *BAT1*, a putative acyltransferase, and modulates brassinosteroid levels (Choi et al. 2013). ARF6 and ARF8 regulate floral organ development in *Arabidopsis*. The double-null mutant *arf6 arf8* arrests flower development, leading to infertile closed buds with short petals, short stamen filaments, and non-dehisced anthers (Nagpal et al. 2005; Tabata et al. 2010).

In rice, OsARF1 was shown to be essential for growth in vegetative organs and seed development (Attia et al. 2009; Waller et al. 2002). *OsARF2*, together with *DROOPING LEAF*, promotes awn development in rice (Toriba and Hirano 2014). ARF12 and OsARF25 regulate root elongation and affects iron accumulation (Qi et al. 2012). OsARF16 is involved in regulating auxin redistribution, phosphate starvation response, and iron deficiency (Shen et al. 2014, 2015). OsARF23 and OsARF24 control cell growth by regulating the actin-binding protein RMD (Li et al. 2014). Zhang et al. (2015) reported that *OsARF19*-overexpressing lines can increase leaf angles by enhancing BR signaling. Meanwhile, the overexpression line of *OsARF19* also showed slender seeds, narrow leaves, and dwarfism (Zhang et al. 2015).

Even though several studies on the relationship of auxin and floral organ development have been reported in *Arabidopsis*, the detailed mechanisms in rice are far from conclusive. In this study, we isolated a T-DNA insertion mutant that displayed abnormal florets as well as altered plant architecture. PCR and quantitative real-time PCR (qRT-PCR) analyses indicated that the T-DNA was inserted into gene *OsARF19* (LOC_Os06g48950), blocking its transcription. To confirm the function of OsARF19 affecting those phenotypes, we generated transgenic plants by knocking down the transcription level of *OsARF19*. Knockdown lines displayed similar phenotypes to the T-DNA insertion mutant. We also determined the expression patterns and subcellular localization of *OsARF19*, which was expressed mainly in young florets, leaves, lamina joint, and elongated basal internodes, and functioned in the nucleus. The combination of morphological and transcription analyses showed that OsARF19 plays important roles in floral organ development, internode elongation, and leaf morphogenesis.

Materials and Methods

Plant Materials and Growth Conditions

The *osarf19* mutant was identified by abnormal florets and enhanced plant height from 400T-DNA tagged lines generated in *O. sativa* var. *japonica* cv. Dongjin, seeds of which were donated by Professor Gynheung An, Crop Biotech Institute, Kyung Hee University, Korea (Jeon et al. 2000; Jeong et al. 2002, 2006). Plants were grown to maturity in the experimental field at Nanjing Agricultural University (Nanjing, China) in the normal growing season.

Cellular Morphology Analysis

Fourth internodes and 3rd leaves counted from the top of wild-type and *osarf19* plants were collected after heading. Samples were fixed in FAA (10 % formalin, 50 % ethanol, and 5 % acetic acid) and dehydrated in a graded ethanol series (Li et al. 2006). For histological analysis, tissues were infiltrated with xylene and embedded in paraplast plus. Materials were sectioned and viewed with a Leica light microscope (DFC402C). Scanning electron microscopy was performed with a JSM-6360LV (Jeol) as described previously (Li et al. 2006).

Genotyping

We obtained flanking sequence information for mutants from OryGenesDB (http://orygenesdb.cirad.fr/). Confirmation of the insertion site was performed by PCR, carried out in a 50-μl mixture containing 20 ng genomic DNA of wild type (WT) and mutant, 0.2 mM dNTP, 0.5 units of Taq polymerase (TaKaRa), 1 mM primers, and 5 μl 10×Taq buffer. PCR was performed as follows: 95 °C for 5 min, followed by 33 cycles of 95 °C for 30 s, annealing for 30 s, 72 °C for 40 s, and a final elongation step at 72 °C for 5 min. The gene-specific primers were P1 (5'-TTGTAAGCGGCAAGAGG-3'), P2

(5'-CCATTTATGGAAAAGTGAG-3'), and P3 (5'-ATCAATTCCACAGTTTTCG-3').

Plasmid Construction, Plant Transformation, and GUS Staining

A 230-bp cDNA fragment of *OsARF19* sequence was amplified using primers OsARF19R1-F (5'-GGGGTACCCCG ATGAGGACATTCACCAAGG-3'), OsARF19R1-R (5'-CCGAGCTCGGTTCACGCAACCGACAAA-3'), OsARF19R2-F (5'-AACTGCAGAATTCAC GCAACCGACAAA-3'), and OsARF19R2-R (5'-CGGGATCCCGGATGAGGACATTCACCAAGG-3') and products were subcloned into the binary vector LH-FAD2-1390RNAi. The LH-FAD2-1390RNAi plasmids were introduced into *Agrobacterium tumefaciens* strain EHA105 by heat shock, and the rice cv. Dongjin was transformed in accordance with a previously published method (Hiei et al. 1994). A 1.4-kb genomic promoter fragment upstream of the ATG start codon was amplified by PCR using Dongjin genomic DNA as the template and cloned into the binary vector pCAMBIA1305 to drive the beta-glucuronidase (GUS) reporter gene expression. The gene-specific primers were GUSF (5'-CCATGATTACGAATTCGCTCGTGCCAGTG AGATTA-3') and GUSR (5'-TTGGCTGCAGGTCGACTC TCTCACTTCTGCTCCCA-3'). Transgenic plants were generated as described above. GUS histochemical staining was performed as described previously (Ma et al. 2012). Images were captured using Leica Application Suite 3.3.

RNA Isolation and Quantitative Real-Time PCR Analysis (qRT-PCR)

Total RNA samples were extracted from young leaves and young roots of 2-week-old seedlings, shoot apices of 1-month-old seedlings, mature leaves, mature roots, leaf sheaths, culms, mature seeds, and panicles during the floret organ development stage of wild type and *osarf19* using an RNA Prep Pure Plant Kit (Tiangen Co., Beijing) and reverse transcribed using a SuperScript II Kit (TaKaRa). QRT-PCR was performed using an SYBR Premix Ex TaqTM Kit (TaKaRa) on an ABI Prism 7500 real-time PCR system with the actin gene used as an internal control. The 2-DDCT method was used to analyze relative changes in gene expression (Livak and Schmittgen 2001). All qRT-PCR primers used for cell cycles genes (*KN*, *H1*, *MCN2*, *MCN3*, *CYCT1*, *CDT2*, *CYCD4*, *CDC20*, *CDKA1*,*CDKA2*, *CAK1*, *CAK1A*, *CDKB*, *E2F2*, *CYCA2.1*, *CYCA2.2*, *CYCA2.3*), cell wall synthesis genes (*CESA6*, *IRX10L*, *GT8*, *UGA4e*, *CSLF6*), rice *PIN* family genes (*OsPIN1a*, *OsPIN1b*, *OsPIN2*, *OsPIN5a*, *OsPIN5b*, *OsPIN8*, *OsPIN9*, *OsPIN10a*), *OsYUCCAs* (*OsYUCCA1*, *2*, *3*, *4*, *5*, *6*, *7*), *OsGHs* (*OsGH3.7*, 3.*8*, 3.9, 3.*10*, 3.*11*, 3.*12*), ABC model-related genes (*OsMADS22*, *OsMADS29*, *OsMADS18*, *OsMADS3*, *OsMADS2*, *CFO1*, *OsMADS1*), *OsARF1-25*, and *OsActin* are listed in Supplementary Table 1.

Subcellular Localization of OsARF19

To determine the cellular localization of OsARF19, green fluorescent protein (GFP) was fused to the C-terminus of OsARF19 under control of the 35S promoter in the pAN580 vector. The gene-specific primers were OsARF19–GFPF (5'-GCCCAGATCAACTAGTATGATGAAGCAGGCGCAGC-AGC-3') and OsARF19–GFPR (5'-CGGACTTA AGACTAGTCGCAGTATTCCAATACCTG-3'). The nuclear marker Ghd7–mCherry was constructed using primers Ghd7–mCherryF (5'-CGGAGCTAGCTCTAGAATG TCGATGGGACCAGCAGC-3') and Ghd7–mCherryR (5'-TCGAGACGTCTCTAGATCTGAACCATT GTCCAAGC-3'). The OsARF19–GFP fusion and GFP were transiently co-transferred into rice protoplasts with the Ghd7–mCherry constructs as described by Bart et al. (2006). Fluorescence images were observed using a Zeiss LSM510 confocal laser microscope.

IAA Treatment

Seeds were surface sterilized with 5.0 % NaClO for 10 min, washed three times with sterilized water, and germinated on wet plates in a 35 °C growth chamber for 3 days. After germination, seedlings were moved to plates containing 0.1 μM indole-3-acetic acid (IAA) solution for 0, 10 min, 30 min, 1 h, 3 h, and 6 h. All samples were used for mRNA extraction and RT-PCR analysis as described above.

Results

Identification of the Mutant *Osarf19*

To elucidate important factors involved in floral organ development, we screened 400T-DNA tagged lines and identified one mutant with partially abnormal florets and enhanced plant height. Using FLS (flanking sequence) and T-DNA vector pGA2717 information from OryGenesDB (http://orygenesdb.cirad.fr/) and sequencing, we found the T-DNA segment was integrated into the 8th exon of LOC_Os06g48950, which encodes for *OsARF19* (Fig. 1a). PCR analysis confirmed that the insertion site was homozygous (Fig. 1b). RT-PCR and qRT-PCR results demonstrated that *OsARF19* transcripts barely accumulated in *osarf19* (Fig. 1c, d). We concluded that *osarf19* was a knockout mutant.

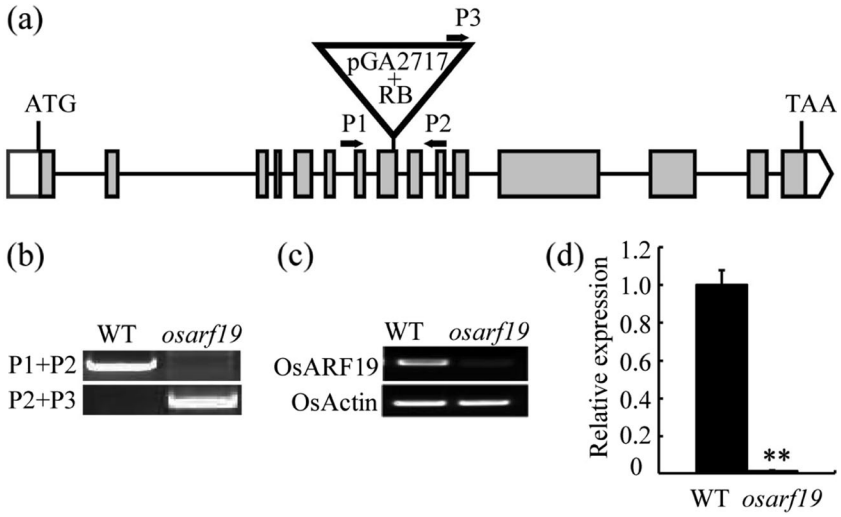

Fig. 1 Identification of the *osarf19* mutation. **a** T-DNA insertion site in mutant *osarf19*. *Triangle* represents the T-DNA vector. The *grey box* represents the exon, and the *black line* represents the intron. P1, P2, and P3 are primers for insertion site determination. **b** PCR analysis to confirm the integration of T-DNA into *OsARF19*. The *upper band* indicates the *OsARF19* gene fragment, and the *lower band* indicates the T-DNA insertion fragment. **c** Reverse transcription PCR analysis to confirm the knockout status of *osarf19*. The *upper bands* show *OsARF19* expression (32 cycles) in wild type (*WT*) and mutant, respectively, and the *bottom bands* show *OsActin* (30 cycles) expression as the control. **d** Quantitative real-time RT-PCR analysis to confirm the knockout status of *osarf19*. Values are given as mean±SD (n=3). *Double asterisk* indicate significant difference between WT and *osarf19* at P=0.01 by Student's t test

Osarf19 Displayed Abnormal Floral Organs, and Altered Plant Height, Leaf Shape, and Seed Size

Compared with wild type (*O. sativa* var. *japonica* cv. Dongjin), most of the *osarf19* florets normally developed, yet the others displayed three types of abnormalities (Fig. 2a–l). The first was an additional lemma-like organ on the same side of palea (Fig. 2e, f), accompanied by a crack when harvested (Fig. 2o). The second was an enlarged palea with a curved tip (Fig. 2g, h), generating an unclosed floret. And the third was variably degenerated paleas, from slight degeneration to complete loss (Fig. 2i–l). The heterozygous plants showed no abnormal florets, similar to WT (Table 1). The abnormal paleas and lemmas could still be observed when mature seeds were harvested (Fig. 2m–q). Each type of abnormal florets only possessed a relatively low proportion, but that was significantly different from WT (Table 1).

The homozygous mutant *osarf19* showed an enlarged plant architecture in all development stages, including the tiller stage (Supplementary Fig. 1) and rice filling stage (Fig. 2r). The heterozygotes showed no obvious differences with WT in plant architecture (Supplementary Fig. 1). Plant height of *osarf19* was slightly increased due to elongated culm internodes (Fig. 2s), especially the basal internode that was much longer than that of WT (Fig. 2s, t). Fifth, 4th, 3rd, and 2nd internodes of *osarf19* were twice, 94 %, 58 %, and 25 % longer than those of WT, respectively, whereas the 1st internodes and panicles were almost the same (Fig. 2t). Similarly, the leaves of *osarf19* had a more slender phenotype. The 2nd and 3rd uppermost leaves showed significantly increased length (Supplementary Fig. 2a, c), whereas the 1st and 2nd leaves slightly decreased in width (Supplementary Fig. 2b, d).

Besides, we investigated other agronomic traits of the *osarf19* mutant. Seed width and thickness were obviously decreased in both de-hulled and hulled grains (Table 2), but seed length was similar to WT (Table 2). One thousand-grain weight significantly reduced and seed set of *osarf19* (84.14±1.25 %) was also lower than WT (94.09±1.8 %), especially in abnormal florets. Unlike the additional lemma-type florets (84.32±4.21 %), the enlarged palea (11.64±6.22 %) and degenerated palea (50.32±10.4 %) type florets were more infertile than normal florets of *osarf19* (Table 2). Panicle number/plant and seed number/plant for *osarf19* were both comparable to those of WT (Table 2). Besides, we detect the phenotypes of a F_2 population of 210 individuals derived from a cross of *osarf19* and WT. In the F_2 population, there were 47 individuals exhibiting similar phenotypes to *osarf19*. The ratio of normal plants to abnormal ones fit a 3:1 ratio which indicated a monogenic inheritance of the mutation. The abnormal phenotypes co-segregated with homozygous T-DNA insertion fragments. The overall results indicated that OsARF19 was related to floret development and plant architecture, as well as affecting yield traits.

RNAi Lines of *OsARF19* Display Similar Phenotypes to Knockout Mutant *Osarf19*

To verify that the mutant phenotypes were due to disruption of *OsARF19*, we first tried to construct a complementary vector, but in vain. We failed to get a positive clone after amplifying nearly 10-kb genome fragments and trying to recombinate them to complementary vector. Instead, we generated

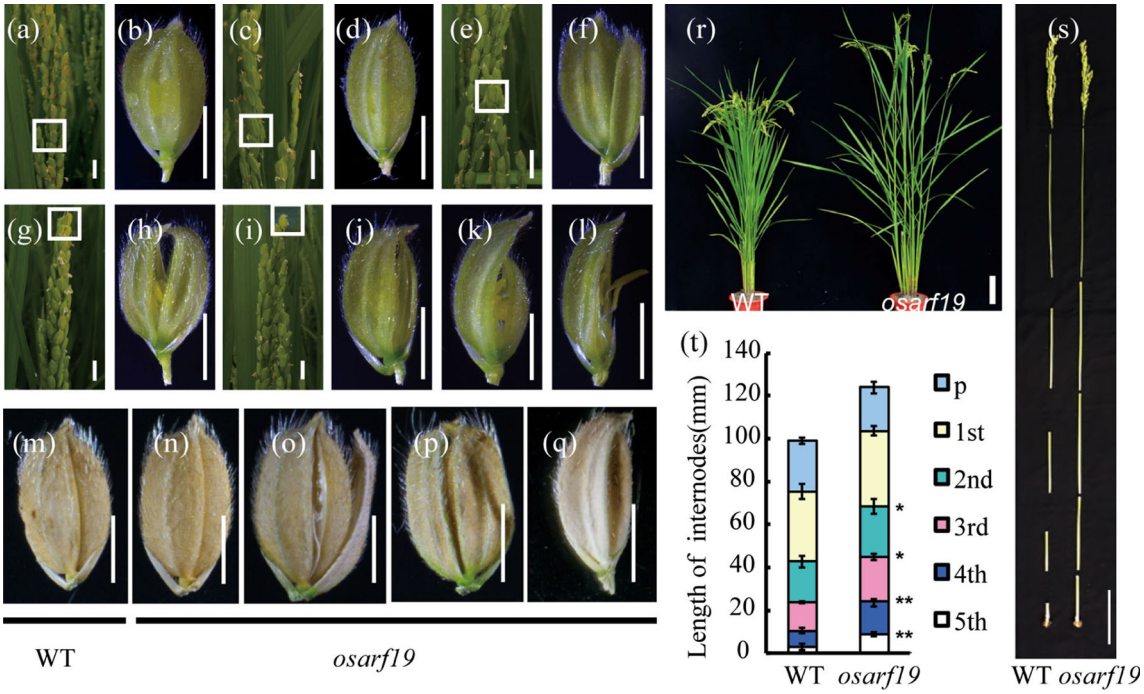

Fig. 2 Disruption of *OsARF19* affected floral organ development and increased plant height. **a** Floret in the wild type (WT) panicle, *bar*=10 mm. **b** Floret of wild type (WT), *bar*=3 mm. **c** Normal floret in the *osarf19* panicle, *bar*=10 mm. **d** Normal floret of the *osarf19*, *bar*=3 mm. **e** Floret with additional lemma in the *osarf19* panicle, *bar*=10 mm. **f** Floret with additional lemma of *osarf19*, *bar*=3 mm. **g** Floret with enlarged palea in the o*sarf19* panicle, *bar*=10 mm. **h** Floret with enlarged palea of *osarf19*, *bar*=3 mm. **i** Florets with degenerated palea in the *osarf19* panicle, *bar*=10 mm. **j–l** Florets with degenerated palea of *osarf19*, *bar*=3 mm. **m** Mature grain from normal florets of wild type (WT). **n** Mature grain from normal florets of *osarf19*. **o** Mature grain from florets with additional lemma in *osarf19*. **p** Mature grains from florets with enlarged palea in *osarf19*. **q** Mature grain from florets with degenerate palea in *osarf19*, **m–q** *bar*=3 mm. **r** Wild type and *osarf19* plants after heading, *bar*=10 cm. **s** Individual culm internode and panicle of wild type (WT) and *osarf19* after heading, bar=10 cm. **t** Lengths of individual culm internode and panicle of wild type (WT) and *osarf19* after heading. Values are means±SD (n=3). *Double asterisk* and *asterisk* indicate significant differences between WT and *osarf19* at P=0.05 and P=0.01 by Student's t test

transgenic plants carrying an *OsARF19* RNA interference (RNAi) construct (Fig. 3h). A plasmid containing two 230-bp fragments of *OsARF19* cDNA inserted in forward and reverse orientations into the LH–1390–RNAi vector was introduced into cv. Dongjin. We obtained positively knockdown (RNAi-8) and empty vector (Vc) lines for function analyses. Compared with the Vc lines, RNAi-8 showed significantly reduced transcripts of *OsARF19* (Fig. 3g). Then, we examined the floret development in both lines. Similar to the *osarf19*, most of florets in the RNAi-8 line were normally organized, but a small proportion displayed abnormalities as shown in Fig. 3b–f. All three types of abnormal florets (an additional lemma, an enlarged palea, and a degenerated palea) were observed in RNAi-8 (Fig. 3d–f). These results confirmed that repression of *OsARF19* was indeed the cause of abnormal floral organ development in the *osarf19* mutant.

Despite abnormalities, the RNAi-8 plant showed accelerated growth rate and increased plant height at the heading stage (Fig. 3a). The knockdown line showed a more slender architecture compared with the Vc line. Harvested seeds of the RNAi line also displayed a slender shape; seed length was almost the same to that of Vc, but the width was significantly reduced (Supplementary Fig. 3a–d). These mutant phenotypes simulated the effects of reduced *OsARF19* transcripts and confirmed that the various phenotypic alterations in the *osarf19* mutant were caused by diminished *OsARF19* expression.

Table 1 Percentages of three types of abnormal florets in wild type, *osarf19*, and heterozygotes

Genotype (n)	Degenerated palea-type floret	Additional lemma-type floret	Enlarged palea-type floret
Wild type (10)	0	0	0
osarf19 (10)	1.91±1.56 %**	2.59±1.53 %**	1.58±1.17 %**
Heterozygote (10)	0	0	0

Values represent means±standard deviation. Numbers in parentheses represent numbers of panicles scored

**Significant differences from wild type by Student' s t test, P<0.01

Table 2 Comparison of agronomic traits between wild type (WT) and *osarf19*

Trait	WT	*osarf19*	*P* value
Plant height (cm)	98.75±7.09	125±4.55**	1.44×10^{-3}
No. of tillers per plant	9.2±2.4	10.90±3.31	0.23
Fertility of normal florets (%)	94.09±1.8	84.14±1.25**	4×10^{-3}
Fertility of florets with enlarged paleas (%)	–	11.64±6.22**	9.31×10^{-11}
Fertility of florets with additional lemmas (%)	–	84.32±4.21**	1.4×10^{-3}
Fertility of florets with degenerated paleas (%)	–	50.32±10.4**	2.59×10^{-5}
No. of days to heading	84.23±1.40	86.22±2.21	0.147
No. of grains (per main panicle)	137.44±7.31	130.60±12.91	0.79
Panicle length (cm)	23.65±1.41	20.35±2.75	0.128
1000-grain weight (g)	28.84±1.75	24.30±0.19**	6.4×10^{-4}
De-hulled grain length (mm)	7.24±0.24	7.33±0.24	6.9×10^{-2}
De-hulled grain width (mm)	3.29±0.16	3.19±0.13**	9×10^{-3}
De-hulled grain thickness (mm)	3.19±0.13	2.08±0.09**	9.358×10^{-11}
Hulled grain length (mm)	5.29±0.18	5.38±0.12	5.2×10^{-2}
Hulled grain width (mm)	2.95±0.11	2.9±0.07**	7×10^{-3}
Hulled grain thickness (mm)	2.08±0.07	1.90±0.06**	7.92×10^{-14}

Fertilities of abnormal florets of *osarf19* were compared with normal florets of wild type (WT). Values represent means (20 samples)±standard deviation

**Significant differences from wild type (WT) by Student's *t* test, $P<0.01$

Mutation in *OsARF19* Increases Cell Elongation

Regulation of cell proliferation and expansion is essential for organ growth (Duan et al. 2014; Horiguchi et al. 2006; Potter and Xu 2001; Sugimoto-Shirasu and Roberts 2003). The enlarged basal internodes and leaves of the *osarf19* mutant prompted us to study how OsARF19 affects organ size. We firstly investigated whether cell length or cell number was the cause of the enlarged phenotypes. We investigated cell size in the 4th internode and 3rd leaf. As shown in Fig. 4a–d, cells in

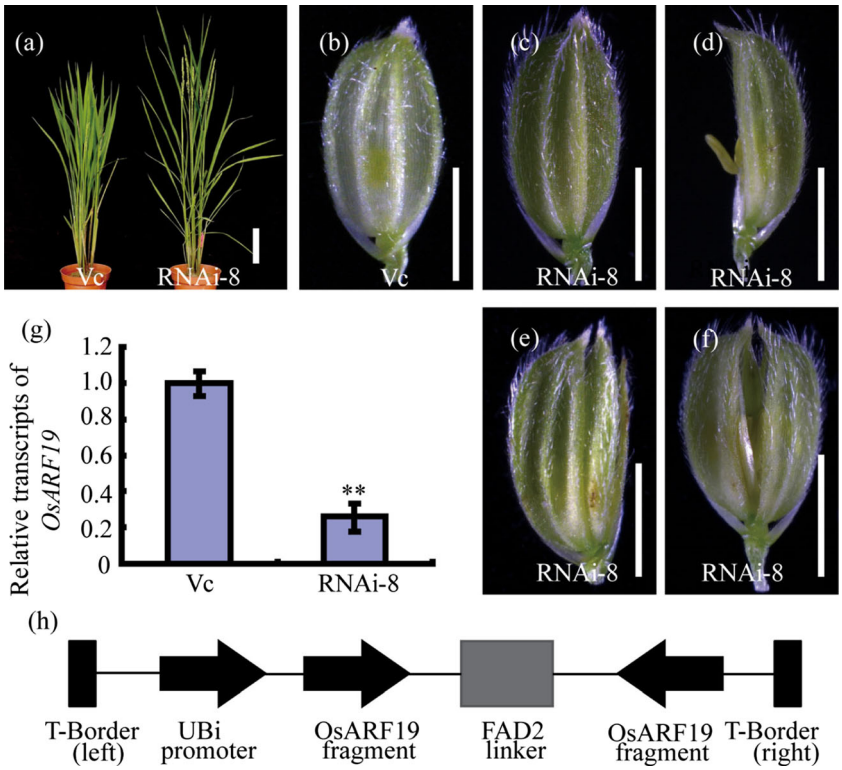

Fig. 3 Phenotypes of the *OsARF19*–RNAi line. **a** Positive *OsARF19* knockdown (RNAi-8) and empty vector (Vc) lines at the heading stage, *bar*=10 cm. **b** Floret from the Vc line, *bar*=3 mm. **c** Normal florets from RNAi–8, *bar*=3 mm. **d**–**f** Three abnormal floret types of RNAi–8 lines, floret with degenerate palea (**d**), additional lemma (**e**), and enlarged palea (**f**) from RNAi–8, *bar*=5 mm. **g** Relative expression levels of *OsARF19* in Vc and RNAi–8 lines. **h** Schematic diagram of *OsARF19*–RNAi construct. FAD2 linker, the intron of *Arabidopsis FAD2* gene (At3g12120.1). UBi promoter, maize *ubi* promoter. Values are means±SD (n=3). *Double asterisk* and *asterisk* indicate significant differences between WT and *osarf19* at P=0.05 and P=0.01 by Student's *t* test

the 4th internode of *osarf19* were almost twice the size of those in WT. Cells in the 3rd leaf of *osarf19* were also longer than in WT (Supplementary Fig. 4).

As the cell wall is the major factor restricting cell elongation, many genes involved in cell wall synthesis are reported to regulate cell elongation. We investigated the expression levels of genes previously identified to be involved in cell wall synthesis (Ning et al. 2011). Our data showed expression levels of *CESA6*, *IRX10L*, *GT8*, *UGA4e*, and *CSLF6* were significantly upregulated in *osarf19* (Fig. 4f). Along with the morphological observations, this indicated that the enlarged plant architecture in *osarf19* was caused by cell elongation. To eliminate the possibility of increased cell number in *osarf19*, we studied the expression levels of some cell cycle regulators in WT and the mutant (Li et al. 2011b). Expression of most of these genes did not differ significantly between WT and the mutant (Fig. 4g). In fact seven genes were significantly downregulated in *osarf19*, indicating that cell proliferation might be retarded (Fig. 4g). These results further confirmed that cell elongation rather than cell proliferation was the cause of the enlarged plant architecture.

OsARF19 Expression Pattern and Subcellular Localization

Since the mutant phenotypes of *osarf19* were involved in both vegetative and reproductive tissues, we expected that transcripts of *OsARF19* would be ubiquitous. We studied the expression patterns of *OsARF19* by qRT-PCR. *OsARF19* transcripts were present in various tissues, but preferentially in the leaves, lamina joint, basal internodes, young panicles or florets, and roots (Fig. 5m). The transcripts in internodes and

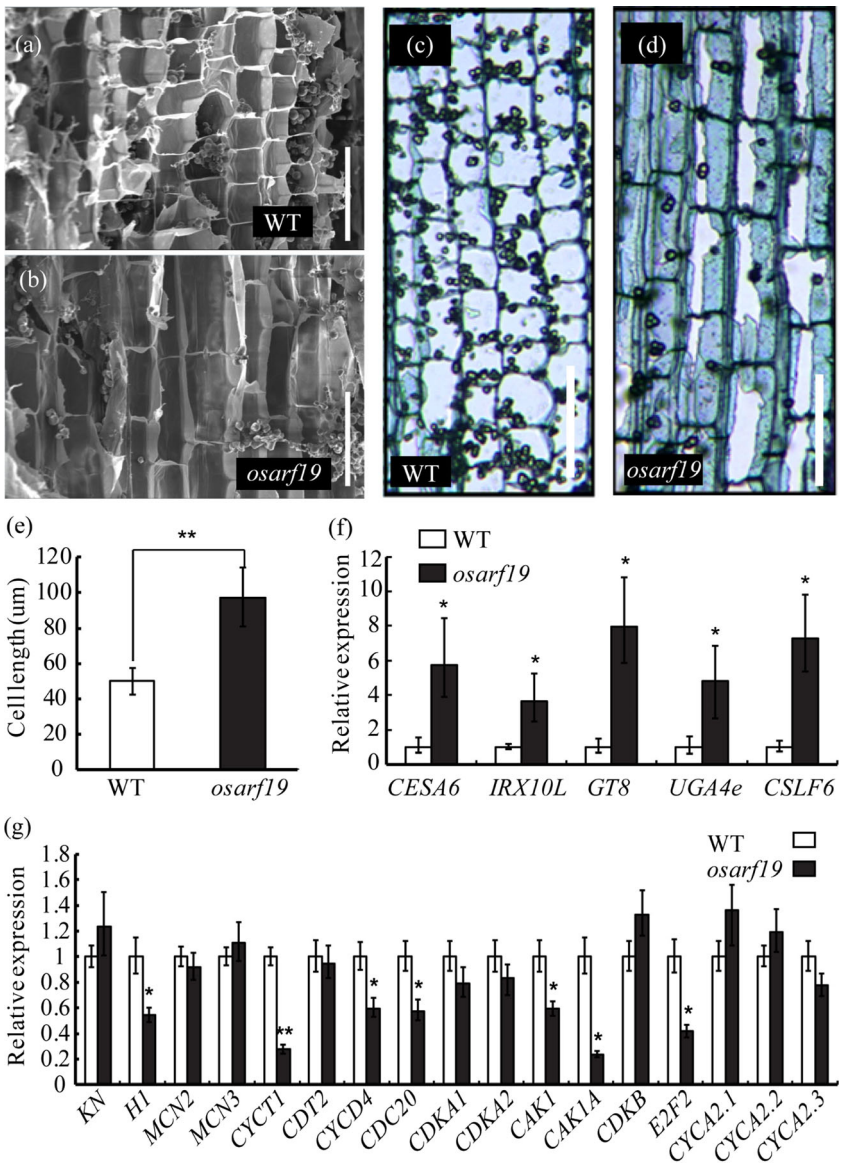

Fig. 4 *Osarf19* enhanced cell elongation in internodes. **a** Inner epidermal cells of a 4th elongated internode from wild type (WT) observed by scanning electron microscope (SEM). **b** Inner epidermal cells of a 4th elongated internode from *osarf19* observed by scanning electron microscope (SEM). **c** Longitudinal section of a 4th elongated internode from wild type (WT). **d** Longitudinal section of a 4th elongated internode from *osarf19*. **e** Average lengths of inner epidermal cells of 4th internodes in wild type (WT) and *osarf19*. **f** Relative expression levels of cell wall synthesis-related genes, *CESA6*, *IRX10L*, *GT8*, *UGA4e*, and *CSLF6*. **g** Relative expression levels of cell cycle-related genes, *KN*, *H1*, *MCN2*, *MCN3*, *CYCT1*,*CDT2*, *CYCD4*, *CDC20*, *CDKA1*,*CDKA2*, *CAK1*, *CAK1A*, *CDKB*, *E2F2*, *CYCA2.1*, *CYCA2.2*, and *CYCA2.3*. Values are mean±SD (n=3). *Double asterisk* and *asterisk* indicate significant differences between WT and *osarf19* at P=0.05 and P=0.01 by Student's t test, **a**–**d**, *bar*=100 um

panicles slowly decreased during maturation of the plant, and *OsARF19* transcripts were barely detectable in mature seeds (Fig. 5m). To further determine spatial expression patterns of *OsARF19*, we generated transgenic plants that contained *OsARF19* promoter::*GUS* fusions. GUS activities were observed in young panicles, culm internodes, leaf sheaths, leaf blades, lamina joint, stamens, and the primary root (Fig. 5a–k). Higher GUS activity was detected in the basal elongated internodes than the upper ones (Fig. 5a–d). Thus, *OsARF19* is a temporally and spatially regulated gene. The abundant transcripts of *OsARF19* in specific tissues were consistent with influencing roles in stem, leaf, and floral organ development.

We also analyzed *OsARF19* transcription in plants treated with 0.1 μM IAA. *OsARF19* expression was rapidly induced by IAA, peaked at 3 h, and subsequently decreased (Fig. 5l). Thus, OsARF19 is an auxin-dependent regulator, in agreement with its roles in auxin signaling.

To investigate subcellular localization of OsARF19, an OsARF19–GFP (green fluorescent protein) fusion protein and the GHD7–mCherry fusion protein (a nuclear marker) were constructed and co-transfected into rice leaf protoplasts (Xue et al. 2008). OsARF19 co-localized with the nuclear-located GHD7 protein and thus functioned in the nucleus (Fig. 5n).

OsARF19 is Involved in Floral Organ Development

Intensive research has shown that auxin controls plant morphogenesis in a concentration-dependent manner (Friml et al. 2002; Habets and Offringa 2014). The abnormal floret organization, together with enlarged plant architecture, promoted us to determine whether the local auxin concentration and responses were changed in *osarf19*. We studied the expression of some key regulators involved in endogenous auxin synthesis, deactivation, and distribution. Previous research has shown *YUCCA* family genes catalyzing tryptamine to N-hydroxytryptamine are responsible for auxin synthesis (Cheng et al. 2007; Stepanova et al. 2008; Zhao 2008). The *GH* family members modulate the adenylation of IAA, and reduce free IAA content (Jain et al. 2006; Takase et al. 2004; Tian et al. 2004). As showed, genes involved in auxin synthesis (*OsYUCCA2*, *5*, *7*) were upregulated, and those involved in auxin deactivation *(OsGH3. 8*, *3. 9*, *3.10*, *3.12)* had reduced activities in *osarf19* (Fig. 6a, b). Additionally, the *PIN* family members can determine local auxin concentration by mediating intercellular transport (Ding and Friml 2010; Qi et al. 2012), and our results showed *OsPIN1b*, *OsPIN5b*, *OsPIN8*, and *OsPIN10a* were greatly upregulated expressed in the *osarf19* (Fig. 6c). Thus, the overall results indicated that the auxin concentration had been increased in *osarf19*. To further test this idea, we examined whether the auxin signaling was activated in the *osarf19* background. By detecting expression of all *OsARFs* (except *OsARF19*), ten members (*OsARF4*, *9*, *10*, *11*, *13*, *14*, *15*, *18*, *20*, *24*) in *osarf19* showed significantly upregulated and the others unchanged (Supplementary Fig. 5).

We questioned whether such enhanced auxin performance would result in altered expression of floral organ regulators, thus leading to abnormal florets according to the ABC model by qRT-PCR analyses (Kobayashi et al. 2012; Li et al. 2011a; Nayar et al. 2013; Prasad et al. 2005; Sang et al. 2012; Sentoku et al. 2005). As shown in Fig. 6d, the expression levels of those regulators showed no significant difference in normal florets of WT and *osarf19*, except that *OsMADS29* was mildly upregulated in the mutant. Interestingly, in abnormal florets, two genes (*OsMDAS29*, *OsMDAS22*) were markedly upregulated compared with WT, and another two genes (*CFO1*, *OsMADS3*) showed slight upregulation, while the others unchanged. Besides, auxin response elements (AuxREs, TGTCTC) were detected in the promoters of *OsMADS29*, *22*, *3*, and *CFO1* (data not shown) which indicated their function might be affected by ARFs (Ulmasov et al. 1997a, b). An earlier report showed that ectopic expression of *OsMADS29* and *OsMADS22* in transgenic rice plants resulted in aberrant floral morphogenesis with a disorganized palea (Nayar et al. 2013;Sentoku et al. 2005), which was similar to the observations in *osarf19*. These results suggest that abnormal floret formation is at least partially caused by altered expression of *OsMADS29* and *OsMADS22*, possibly resulting from irregular local auxin concentration and responses (Fig. 6a).

Discussion

The plant hormone auxin is an essential regulator of normal growth and development (Blakeslee et al. 2005). It can exert pleiotropic effects on development by regulating very basic processes such as cell division, growth, and differentiation (Benkova et al. 2003; Friml et al. 2002; Habets and Offringa 2014). These effects are always mediated by Aux/IAA protein degradation and subsequently auxin response factor (ARF) activation (Guilfoyle and Hagen 2007). In this study, we identified a T-DNA insertion mutant, *osarf19*, in which *OsARF19* transcription was blocked (Fig. 1a–d). The mutant displayed

Fig. 5 Expression pattern and subcellular localization of *OsARF19*. **a**–**k** ▶ GUS staining of various tissues from *OsARF19*pro::GUS transgenic lines, *bar*=5 mm. **l** *OsARF19* transcription levels after 0, 15, 30, 1, 3, and 6 h of 10 uM IAA treatment. **m** *OsARF19* transcription levels in various tissues, viz. 1st elongated internode, 3rd elongated internode, 4th elongated internode, young leaf blades, mature leaf blades, lamina joint, leaf sheath, panicle 1 (panicle before heading), panicle 2 (panicle at heading stage), panicle 3 (panicle after heading), mature seeds, young roots, and mature roots. **n** Subcellular localization of OsARF19–GFP fusion protein and GFP protein. GHD7 was used as a nuclear marker, *bar*=5 um. Values are mean±SD (n=3). *Double asterisk* and *asterisk* indicate significant differences between WT and *osarf19* at P=0.05 and P=0.01 by Student's t test

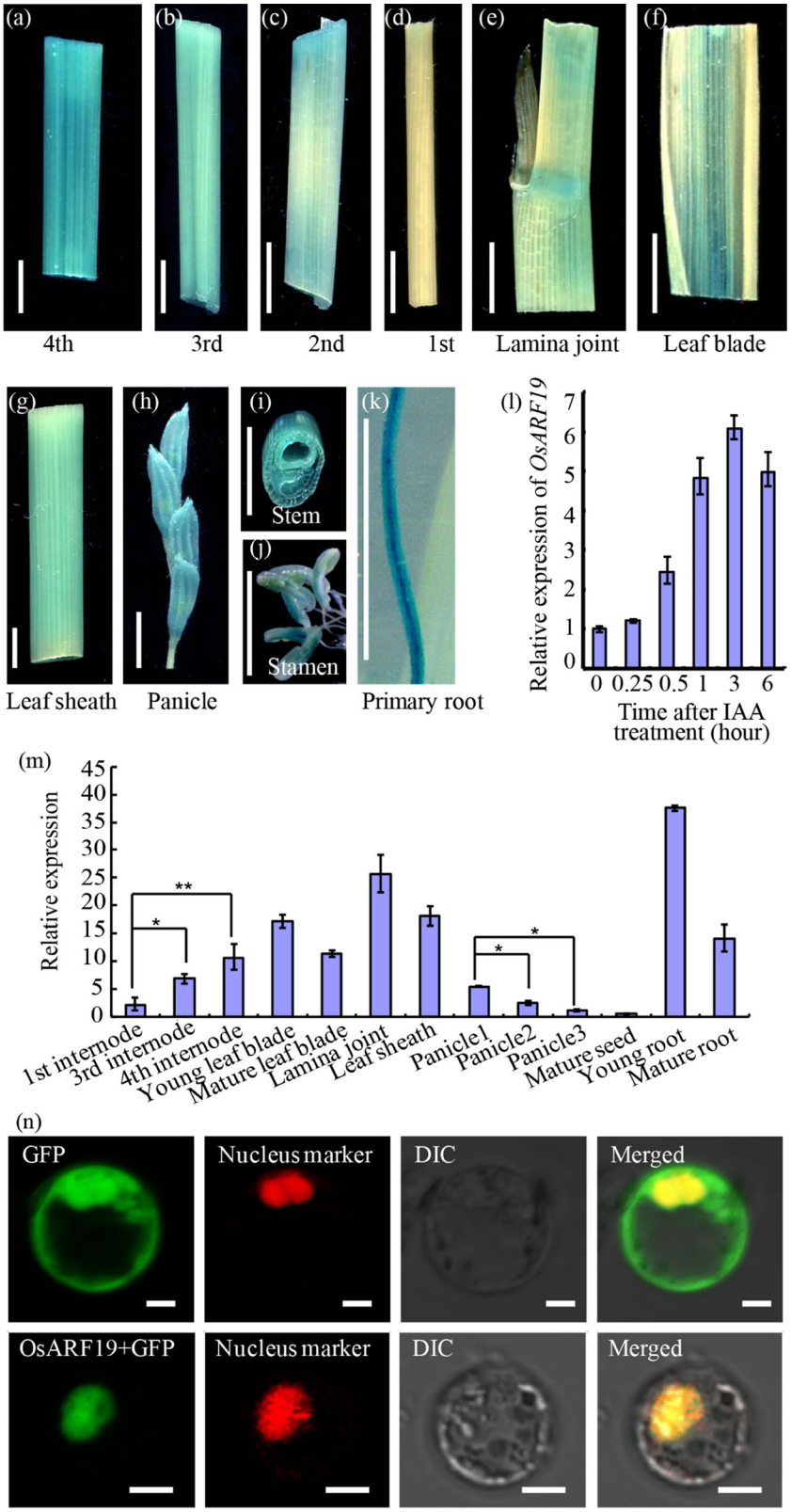

various phenotypes, such as abnormal florets, elongated basal internodes, and altered leaf morphology, indicating *OsARF19* functions in regulating such processes (Fig. 2a–t). Compared with previous reports on roles of *ARF19* in leaf and lateral root development as well as the crosstalk with BR, to our knowledge, this study was firstly to relate OsARF19 with floral

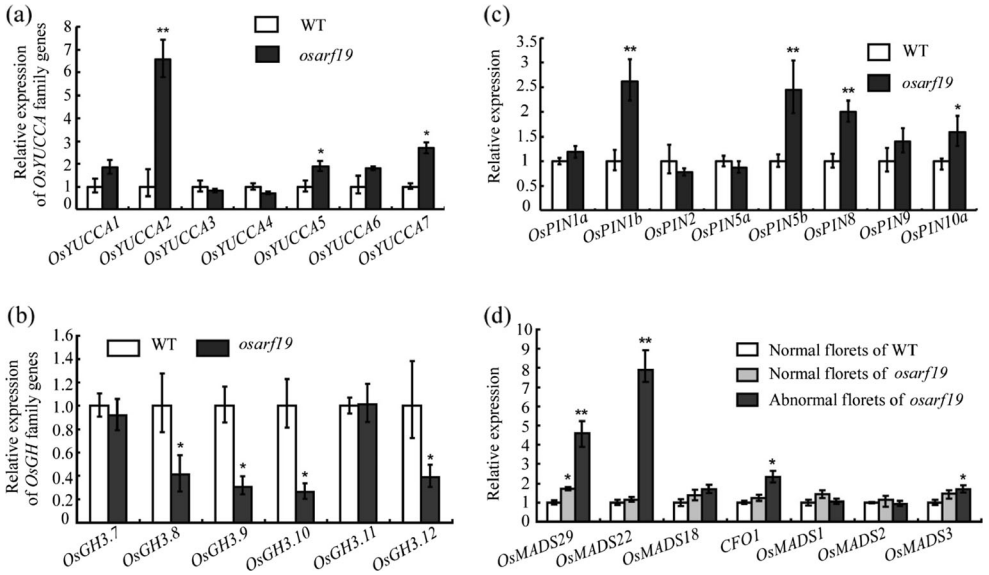

Fig. 6 Expression levels of rice *YUCCA*, *GH*, *PIN* family, and floret formation-related genes in wild type (WT) and *osarf19*. **a** Expression levels of rice *YUCCA* family genes, *OsYUCCA1*, *OsYUCCA2*, *OsYUCCA3*, *OsYUCCA4*, *OsYUCCA5*, *OsYUCCA6*, and *OsYUCCA7* in wild type (WT) and *osarf19*, 2 weeks before heading. **b** Expression levels of rice *GH* family genes, *OsGH3.7*, *OsGH3.8*, *OsGH3.9*, *OsGH3.10*, *OsGH3.11*, and *OsGH3.12* in wild type (WT) and *osarf19*, 2 weeks before heading. **c** Expression levels of rice PIN family genes, *OsPIN1a*, *OsPIN1b*, *OsPIN2*, *OsPIN5a*, *OsPIN5b*, *OsPIN8*, *OsPIN9*, and *OsPIN10a* in wild type (WT) and *osarf19*, 2 weeks before heading. **d** Expression levels of floret formation-related genes, *OsMADS29*, *OsMADS22*, *OsMADS18*, *CFO1* (chimeric floral organs1), *OsMADS1*, *OsMADS2*, and *OsMADS3* in normal florets of wild type (WT), *osarf19*, and abnormal florets of *osarf19*. Values are mean±SD (n=3). *Double asterisk* and *asterisk* indicate significant differences between WT and *osarf19* at P=0.05 and P=0.01 by Student's t test

organ development (Choi et al. 2013; Okushima et al. 2007; Wilmoth et al. 2005; Zhang et al. 2015). The increased plant height in *osarf19* was in agreement with the former finding that overexpression of *OsARF19* resulted in a dwarf plant (Zhang et al. 2015). But *OsARF19* knockout and overexpression lines shared similar phenotypes in leaf and seed width, which might be due to a high degree of redundancy among ARF family members in rice (Zhang et al. 2015). Using double-stranded RNA interference (RNAi), we obtained transgenic lines having similar phenotypes to *osarf19* (Fig. 3a–h). These results indicated that the abnormal phenotypes in *osarf19* were indeed caused by disruption of *OsARF19*.

We studied the expression pattern of *OsARF19* by qRT-PCR and GUS staining analyses. *OsARF19* was temporally and spatially expressed with its transcripts mainly in the culm internodes, lamina joint, root, leaves, and florets (Fig. 5m). Such tissue-specific expression pattern might be related with its roles in affecting those organ morphologies. The expression of *OsARF19* in the lamina joint and root was correlated with its function in regulating the leaf angle and lateral root development (Zhang et al. 2015). Additionally, when analysis focused on a particular organ (such as the culm internodes), transcripts always peaked at an early stage and gradually decreased during maturation (Fig. 5a–d). The elongation of basal rather than uppermost internodes were possibly due to such temporally expression pattern. Yamamoto et al. (2007) reported overexpression of the *OsYUCCA* family genes could promote auxin synthesis and basal internode elongation at an early stage, which did not occur in wild type. And suppressing expression of *OsGH3.8* by RNAi also increased auxin content and caused great basal internode elongation, as well as disorganized florets, while the upper ones were less affected (Yadav et al. 2007). We supposed the elongated basal internodes in *osarf19* should result from the high auxin performance, including upregulation of *OsYUCCA*s, *OsPINs*, and downregulation of *OsGH*s (Fig. 6a–c). As is known, control of basal internode length is an important task in plant breeding. The basal internode length and its dry weight content are major plant traits that determine straw strength and correlates with lodging resistance (Islam et al. 2007; Kashiwagi and Ishimaru 2004). The *osarf19* mutant could be useful as an experimental or breeding material to modulate basal internode length for ideal plant architecture.

It is well known that the size of an organ is determined by cell proliferation and expansion, and auxin regulates both processes (Horiguchi et al. 2006; Potter and Xu 2001; Sugimoto-Shirasu and Roberts 2003). In this study, the *osarf19* mutant exhibited obviously longer cells than WT, responsible for elongated basal internode (Fig. 4a–d). Moreover, expression levels of genes involved in cell elongation (e.g., *CESA6*, *IRX10L*, *GT8*, *UGA4e*, and *CSLF6*) were significantly upregulated, further confirming that result. *ARF*s with a glutamine-rich middle region always functioned as activators of auxin-responsive gene expression while *ARF*s with proline- and/or serine-rich middle regions might repress the transcription

activities (Tiwari et al. 2003; Qi et al. 2012). The *OsARF19* containing a glutamine-rich middle region was considered as a transcription activator (Shen et al. 2010). Thus, it was unlikely that the upregulation of cell elongation genes were directly regulated by *OsARF19*, which might be possibly caused by other *OsARFs* enhancement (Supplementary Fig. 5).

Despite the effects of mutation on plant architecture, *OsARF19* is also critical for floral organ development. First, we obtained three types of abnormal florets in both *osarf19* mutant and RNAi lines. Abundant transcripts of *OsARF19* were detected in young panicles, supporting a role in floral organ development (Fig. 5m). Recent studies have demonstrated that auxin controls meristem development in a concentration-dependent manner (Friml 2003; Habets and Offringa 2014). Our findings showed that disruption of *OsARF19* might lead to increased auxin concentration, with upregulated *OsYUCCA*s and downregulated *OsGH*s (Fig. 6a). A recent study demonstrated that *OsARF19* can directly bind to promoter of *OsGH3-5* and reduce free IAA concentration (Zhang et al. 2015). However, whether *OsARF19* could target other *OsGH* members (*OsGH3.8*, *3.9*, *3.10*, *3.12)* and feedback regulation on *OsYUCCA*s and *OsPIN*s is still complex and is worth further investigation.

Meanwhile, the elevated auxin concentration could induce auxin signaling transduction and might alter the expression of downstream genes (Supplementary Fig. 5). According to the ABC model, *OsMADS1* was a Class E gene and played a role in determining the identities of palea and lemma (Jeon et al. 2000). Dysfunction of *OsMADS1* can result in elongated leafy palea and lemma and an unclosed floret. The expression level of *OsMADS1* was not altered in *osarf19*, which was coordinated with that *OsMADS1* functions upstream of *ARFs*. However, another two genes (*OsMADS29*, *OsMADS22*) were markedly upregulated in abnormal florets of *osarf19* (Fig. 6d). AuxREs (TGTCTC) were detected in the promoters of such two genes (data not shown), which further confirmed their transcription was regulated by the auxin signaling pathway.

OsMADS22 is a member of the *STMADS11*-like family of MADS-box genes. Ectopic expression of *OsMADS22* in transgenic rice resulted in different aberrant floral morphogenesis (Sentoku et al. 2005), which were similar to the abnormal floret with an additional lemma and degenerated palea in *osarf19*. *OsMADS29* was induced by auxin, and overexpression of *OsMADS29* caused aberration flower morphology with a small and degenerated palea (Nayar et al. 2013). The elevated *OsMADS29* expression might be correlated with the degenerated palea found in *osarf19*. Therefore, it is possible that the abnormal florets in *osarf19* were due to improper expression of these two genes, and other possible regulators contributing to palea and lemma development could not be discounted (Fig. 6d). And further researches on auxin and such two regulators will be carried out in our future studies.

In this study, new evidence was provided for functions of ARFs in cell elongation and floral organ development. The *osarf19* mutant displayed various phenotypes in both vegetative and reproductive organs, revealing its pleiotropic effects at different development stages. Although previous studies reported that ARFs (ARF5, 6, 8) affect flowering pattern in *Arabidopsis* (Garrett et al. 2012; Nagpal et al. 2005), this is the first report on the effects of *OsARF19* on floral organ development in rice. Our results confirmed previous conclusions on the influence of auxin on floral organ development, but raised new questions as to how ARFs coordinate with each other and what are their downstream targets. Our findings provide an important basis to address those questions.

Acknowledgments This research was supported by the Key Laboratory of Biology, Genetics and Breeding of Japonica Rice in Mid-lower Yangtze River, Ministry of Agriculture of China, The Yangtze River Valley Hybrid Rice Collaboration Innovation Center, Jiangsu Collaborative Innovation Center for Modern Crop Production, and the grants from the 863 Program (2014AA10A603-15), National Science and Technology Support Program (2013BAD01B02-16), Jiangsu Science and Technology Development Program (BE2014394), Jiangsu Province Self- innovation Program (CX(12)1003), and Qing Lan Project.

Author Contributions S.Z. Zhang J.M. Wan, and L. Jiang conceived and designed the experiments. S.Z. Zhang, T. Wu, X. Liu, and S.J. Liu performed the experiments. S.Z. Zhang and T. Wu analyzed the data. J.M. Wan and L. Jiang contributed reagents/materials/analysis tools and revised the paper. S.Z. Zhang wrote the paper.

Compliance with Ethical Standards

Conflict of Interest The authors declare that they have no competing interests.

References

Aida M, Vernoux T, Furutani M, Traas J, Tasaka M (2002) Roles of *PIN-FORMED1* and *MONOPTEROS* in pattern formation of the apical region of the Arabidopsis embryo. Development 129:3965–3974

Attia KA, Abdelkhalik AF, Ammar MH, Wei C, Yang J, Lightfoot DA, El-Sayed WM, El-Shemy HA (2009) Antisense phenotypes reveal a functional expression of OsARF1, an auxin response factor, in transgenic rice. Curr Issues Mol Biol 11(Suppl 1):i29–i34

Bart R, Chern M, Park CJ, Bartley L, Ronald PC (2006) A novel system for gene silencing using siRNAs in rice leaf and stem derived protoplasts. Plant Methods 2:13

Benkova E, Michniewicz M, Sauer M, Teichmann T, Seifertova D, Jurgens G, Friml J (2003) Local, efflux-dependent auxin gradients as a common module for plant organ formation. Cell 115:591–602

Blakeslee JJ, Peer WA, Murphy AS (2005) Auxin transport. Curr Opin Plant Biol 8:494–500

Cai Q, Yuan Z, Chen M, Yin C, Luo Z, Zhao X, Liang W, Hu J, Zhang D (2014) Jasmonic acid regulates spikelet development in rice. 5:3476

Cheng Y, Dai X, Zhao Y (2007) Auxin synthesized by the YUCCA flavinmonooxygenases is essential for embryogenesis and leaf formation in Arabidopsis. Plant Cell 19:2430–2439

Choi S, Cho YH, Kim K, Matsui M, Son SH, Kim SK, Fujioka S, Hwang I (2013) BAT1, a putative acyltransferase, modulates brassinosteroid levels in Arabidopsis. Plant J 73:380–391

Ding Z, Friml J (2010) Auxin regulates distal stem cell differentiation in Arabidopsis roots. Proc Natl Acad Sci U S A 107:12046–12051

Dreni L, Jacchia S, Fornara F, Fornari M, Ouwerkerk PB, An G, Colombo L, Kater MM (2007) The D-lineage MADS-box gene OsMADS13 controls ovule identity in rice. Plant J 52:690–699

Duan P, Rao Y, Zeng D, Yang Y, Xu R, Zhang B, Dong G, Qian Q, Li Y (2014) SMALL GRAIN 1, which encodes a mitogen-activated protein kinase kinase 4, influences grain size in rice. Plant J 77:547–557

Friml J (2003) Auxin transport—shaping the plant. Curr Opin Plant Biol 6:7–12

Friml J, Benkova E, Blilou I, Wisniewska J, Hamann T, Ljung K, Woody S, Sandberg G, Scheres B, Jurgens G, Palme K (2002) AtPIN4 mediates sink-driven auxin gradients and root patterning in Arabidopsis. Cell 108:661–673

Garrett JJ, Meents MJ, Blackshaw MT, Blackshaw LC, Hou H, Styranko DM, Kohalmi SE, Schultz EA (2012) A novel, semi-dominant allele of *MONOPTEROS* provides insight into leaf initiation and vein pattern formation. Planta 236:297–312

Guilfoyle TJ, Hagen G (2007) Auxin response factors. Curr Opin Plant Biol 10:453–460

Habets ME, Offringa R (2014) PIN-driven polar auxin transport in plant developmental plasticity: a key target for environmental and endogenous signals. New Phytol 203:362–377

Hardtke CS, Berleth T (1998) The Arabidopsis gene *MONOPTEROS* encodes a transcription factor mediating embryo axis formation and vascular development. EMBO J 17:1405–1411

Hardtke CS, Ckurshumova W, Vidaurre DP, Singh SA, Stamatiou G, Tiwari SB, Hagen G, Guilfoyle TJ, Berleth T (2004) Overlapping and non-redundant functions of the Arabidopsis auxin response factors MONOPTEROS and NONPHOTOTROPIC HYPOCOTYL 4. Development 131:1089–1100

Hiei Y, Ohta S, Komari T, Kumashiro T (1994) Efficient transformation of rice (*Oryza sativa* L.) mediated by *Agrobacterium* and sequence analysis of the boundaries of the T-DNA. Plant J 6:271–282

Horiguchi G, Ferjani A, Fujikura U, Tsukaya H (2006) Coordination of cell proliferation and cell expansion in the control of leaf size in *Arabidopsis thaliana*. J Plant Res 119:37–42

Islam MS, Peng S, Visperas RM, Ereful N, Bhuiya MSU, Julfiquar AW (2007) Lodging-related morphological traits of hybrid rice in a tropical irrigated ecosystem. Field Crop Res 101:240–248

Jain M, Kaur N, Tyagi AK, Khurana JP (2006) The auxin-responsive *GH3* gene family in rice (*Oryza sativa*). Funct Integr Genomics 6: 36–46

Jeon JS, Lee S, Jung KH, Jun SH, Jeong DH, Lee J, Kim C, Jang S, Yang K, Nam J, An K, Han MJ, Sung RJ, Choi HS, Yu JH, Choi JH, Cho SY, Cha SS, Kim SI, An G (2000) T-DNA insertional mutagenesis for functional genomics in rice. Plant J 22:561–570

Jeong DH, An S, Kang HG, Moon S, Han JJ, Park S, Lee HS, An K, An G (2002) T-DNA insertional mutagenesis for activation tagging in rice. Plant Physiol 130:1636–1644

Jeong D, An S, Park S, Kang H, Park G, Kim S, Sim J, Kim Y, Kim M, Kim S, Kim J, Shin M, Jung M, An G (2006) Generation of a flanking sequence-tag database for activation-tagging lines in japonica rice. Plant J 45:123–132

Kashiwagi T, Ishimaru K (2004) Identification and functional analysis of a locus for improvement of lodging resistance in rice. Plant Physiol 134:676–683

Khanday I, Yadav SR, Vijayraghavan U (2013) Rice *LHS1/OsMADS1* controls floret meristem specification by coordinated regulation of transcription factors and hormone signaling pathways. Plant Physiol 161:1970–1983

Kobayashi K, Yasuno N, Sato Y, Yoda M, Yamazaki R, Kimizu M, Yoshida H, Nagamura Y, Kyozuka J (2012) Inflorescence meristem identity in rice is specified by overlapping functions of three AP1/FUL-like MADS box genes and *PAP2*, a SEPALLATA MADS box gene. Plant Cell 24:1848–1859

Krizek BA, Fletcher JC (2005) Molecular mechanisms of flower development: an armchair guide. Nat Rev Genet 6:688–698

Li N, Zhang DS, Liu HS, Yin CS, Li XX, Liang WQ, Yuan Z, Xu B, Chu HW, Wang J, Wen TQ, Huang H, Luo D, Ma H, Zhang DB (2006) The rice tapetum degeneration retardation gene is required for tapetum degradation and anther development. Plant Cell 18:2999–3014

Li H, Liang W, Hu Y, Zhu L, Yin C, Xu J, Dreni L, Kater MM, Zhang D (2011a) Rice *MADS6* interacts with the floral homeotic genes *SUPERWOMAN1, MADS3, MADS58, MADS13*, and *DROOPING LEAF* in specifying floral organ identities and meristem fate. Plant Cell 23:2536–2552

Li Y, Fan C, Xing Y, Jiang Y, Luo L, Sun L, Shao D, Xu C, Li X, Xiao J, He Y, Zhang Q (2011b) Natural variation in *GS5* plays an important role in regulating grain size and yield in rice. Nat Genet 43:1266–1269

Li G, Liang W, Zhang X, Ren H, Hu J, Bennett MJ, Zhang D (2014) Rice actin-binding protein RMD is a key link in the auxin-actin regulatory loop that controls cell growth. Proc Natl Acad Sci U S A 111: 10377–10382

Livak KJ, Schmittgen TD (2001) Analysis of relative gene expression data using real-time quantitative PCR and the 2(−Delta Delta C(T)) method. Methods 25:402–408

Ma X, Cheng Z, Qin R, Qiu Y, Heng Y, Yang H, Ren Y, Wang X, Bi J, Ma X, Zhang X, Wang J, Lei C, Guo X, Wang J, Wu F, Jiang L, Wang H, Wan J (2012) *OsARG* encodes an arginase that plays critical roles in panicle development and grain production in rice. Plant J 73:190–200

McSteen P (2010) Auxin and monocot development. Cold Spring Harb Perspect Biol 2:a1479

Moon Y, Jung J, Kang H, An G (1999) Identification of a rice *APETALA3* homologue by yeast two-hybrid screening. Plant Mol Biol 40:167–177

Nagpal P, Ellis CM, Weber H, Ploense SE, Barkawi LS, Guilfoyle TJ, Hagen G, Alonso JM, Cohen JD, Farmer EE, Ecker JR, Reed JW (2005) Auxin response factors ARF6 and ARF8 promote jasmonic acid production and flower maturation. Development 132:4107–4118

Nayar S, Sharma R et al (2013) Functional delineation of rice *MADS29* reveals its role in embryo and endosperm development by affecting hormone homeostasis. J Exp Bot 64:4239–4253

Ning J, Zhang B, Wang N, Zhou Y, Xiong L (2011) *Increased leaf angle1*, a Raf-like MAPKKK that interacts with a nuclear protein family, regulates mechanical tissue formation in the Lamina joint of rice. Plant Cell 23:4334–4347

Okushima Y, Fukaki H, Onoda M, Theologis A, Tasaka M (2007) ARF7 and ARF19 regulate lateral root formation via direct activation of *LBD/ASL* genes in Arabidopsis. Plant Cell 19:118–130

Potter CJ, Xu T (2001) Mechanisms of size control. Curr Opin Genet Dev 11:279–286

Prasad K, Parameswaran S et al (2005) *OsMADS1*, a rice MADS-box factor, controls differentiation of specific cell types in the lemma and palea and is an early-acting regulator of inner floral organs. Plant J 43:915–928

Przemeck GK, Mattsson J, Hardtke CS, Sung ZR, Berleth T (1996) Studies on the role of the *Arabidopsis* gene *MONOPTEROS* in vascular development and plant cell axialization. Planta 200:229–237

Qi Y, Wang S, Shen C, Zhang S, Chen Y, Xu Y, Liu Y, Wu Y, Jiang D (2012) *OsARF12*, a transcription activator on auxin response gene, regulates root elongation and affects iron accumulation in rice (*Oryza sativa*). New Phytol 193:109–120

Sang X, Li Y, Luo Z, Ren D, Fang L, Wang N, Zhao F, Ling Y, Yang Z, Liu Y, He G (2012) *CHIMERIC FLORAL ORGANS1*, encoding a

monocot-specific MADS box protein, regulates floral organ identity in rice. Plant Physiol 160:788–807

Sentoku N, Kato H, Kitano H, Imai R (2005) *OsMADS22*, an STMADS11-like MADS-box gene of rice, is expressed in non-vegetative tissues and its ectopic expression induces spikelet meristem indeterminacy. Mol Genet Genomics 273:1–9

Shen C, Wang S et al (2010) Functional analysis of the structural domain of ARF proteins in rice (*Oryza sativa* L.). J Exp Bot 61:3971–3981

Shen CJ, Yue RQ, Yang YJ, Zhang L, Sun T, Tie SG, Wang HZ (2014) OsARF16 is involved in cytokinin-mediated inhibition of phosphate transport and phosphate signaling in rice (*Oryza sativa* L.). Plos One 9:e112906

Shen CJ, Yue RQ, Sun T, Zhang L, Yang YJ, Wang HZ (2015) OsARF16, a transcription factor regulating auxin redistribution, is required for iron deficiency response in rice (*Oryza sativa* L.). Plant Sci 231: 148–158

Stepanova AN, Robertson-Hoyt J, Yun J, Benavente LM, Xie DY, Dolezal K, Schlereth A, Jurgens G, Alonso JM (2008) TAA1-mediated auxin biosynthesis is essential for hormone crosstalk and plant development. Cell 133:177–191

Sugimoto-Shirasu K, Roberts K (2003) "Big it up": endoreduplication and cell-size control in plants. Curr Opin Plant Biol 6:544–553

Tabata R, Ikezaki M, Fujibe T, Aida M, Tian CE, Ueno Y, Yamamoto KT, Machida Y, Nakamura K, Ishiguro S (2010) Arabidopsis auxin response factor6 and 8 regulate jasmonic acid biosynthesis and floral organ development via repression of class 1 *KNOX* genes. Plant Cell Physiol 51:164–175

Takase T, Nakazawa M, Ishikawa A, Kawashima M, Ichikawa T, Takahashi N, Matsui M (2004) *Ydk1-D*, an auxin responsive GH3 mutant that is involved in hypocotyl and root elongation. Plant J 37: 471–483

Theissen G (2001) Development of floral organ identity: stories from the MADS house. Curr Opin Plant Biol 4:75–85

Thompson BE, Hake S (2009) Translational biology: from Arabidopsis flowers to grass inflorescence architecture. Plant Physiol 149:38–45

Tian CE, Muto H, Higuchi K, Matamura T, Tatematsu K, Koshiba T, Yamamoto KT (2004) Disruption and overexpression of auxin response factor 8 gene of Arabidopsis affect hypocotyl elongation and root growth habit, indicating its possible involvement in auxin homeostasis in light condition. Plant J 40:333–343

Tiwari SB, Hagen G, Guilfoyle T (2003) The roles of auxin response factor domains in auxin-responsive transcription. Plant Cell 15: 533–543

Toriba T, Hirano HY (2014) The DROOPING LEAF and OsETTIN2 genes promote awn development in rice. Plant J 77:616–626

Ulmasov T, Hagen G, Guilfoyle TJ (1997a) ARF1, a transcription factor that binds to auxin response elements. Science 276: 1865–1868

Ulmasov T, Murfett J, Hagen G, Guilfoyle TJ (1997b) Aux/IAA proteins repress expression of reporter genes containing natural and highly active synthetic auxin response elements. Plant Cell 9:1963–1971

Waller F, Furuya M, Nick P (2002) OsARF1, an auxin response factor from rice, is auxin-regulated and classifies as a primary auxin responsive gene. Plant Mol Biol 50:415–425

Wilmoth JC, Wang S, Tiwari SB, Joshi AD, Hagen G, Guilfoyle TJ, Alonso JM, Ecker JR, Reed JW (2005) NPH4/ARF7 and ARF19 promote leaf expansion and auxin-induced lateral root formation. Plant J 43:118–130

Xiao H, Wang Y, Liu D, Wang W, Li X, Zhao X, Xu J, Zhai W, Zhu L (2003) Functional analysis of the rice *AP3* homologue *OsMADS16* by RNA interference. Plant Mol Biol 52:957–966

Xue W, Xing Y, Weng X, Zhao Y, Tang W, Wang L, Zhou H, Yu S, Xu C, Li X, Zhang Q (2008) Natural variation in *Ghd7* is an important regulator of heading date and yield potential in rice. Nat Genet 40: 761–767

Yadav SR, Prasad K, Vijayraghavan U (2007) Divergent regulatory *OsMADS2* functions control size, shape and differentiation of the highly derived rice floret second-whorl organ. Genetics 176:283–294

Yamaguchi T, Lee DY, Miyao A, Hirochika H, An G, Hirano HY (2006) Functional diversification of the two C-class MADS box genes *OSMADS3* and *OSMADS58* in *Oryza sativa*. Plant Cell 18:15–28

Yamamoto Y, Kamiya N, Morinaka Y, Matsuoka M, Sazuka T (2007) Auxin biosynthesis by the *YUCCA* genes in rice. Plant Physiol 143: 1362–1371

Zhang S, Wang S, Xu Y, Yu C, Shen C, Qian Q, Geisler M, Jiang DA, Qi Y (2015) The auxin response factor, OsARF19, controls rice leaf angles through positively regulating OsGH3-5 and OsBRI1. Plant Cell Environ 38:638–654

Zhao Y (2008) The role of local biosynthesis of auxin and cytokinin in plant development. Curr Opin Plant Biol 11:16–22